Int. J. Multiphase Flow Vol. 14, No. 6, pp. 765–776, 1988
Printed in Great Britain.

0301-9322/88 $3.00 + 0.00

LASER-DOPPLER MEASUREMENT OF THE VELOCITY AND DIAMETER OF BUBBLES USING THE TRIPLE-PEAK TECHNIQUE

P. Y. W. Yu
Litton Systems Canada Ltd, 25 Cityview Drive, Plant 409, Rexdale, Ontario M9W 5A7, Canada

R. L. Varty†
Department of Mechanical Engineering, University of Alberta, Edmonton, Alberta T6G 2G8, Canada

(*Received* 27 *January* 1988; *in revised form* 1 *July* 1988)

Abstract—The velocity and diameter of nitrogen bubbles rising in quiescent water were simultaneously measured by a dual-beam laser-Doppler anemometer. The range of bubble diameters was 0.8–1.8 mm. The triple-peak technique was used to obtain the bubble diameter from the anemometer signal. Using a single stream of bubbles, the horizontal area of the bubble-detection region was proportional to the square of the bubble diameter. Using additional streams of bubbles to generate an optical disturbance, the probability of detecting a valid signal decreased linearly with increasing bubble flowrate of the additional streams and was independent of their location and number. The maximum void fraction was 0.01.

Key Words: bubble, laser anemometer, laser Doppler, particle size

1. INTRODUCTION

The measurement of bubbly flow using the laser-Doppler anemometer (LDA) is affected by the difference in the refractive indexes of the gas and liquid phases. On one hand, the difference in refractive indexes allows the measurement of the velocity and curvature of the bubble surface. On the other hand, it can produce unwanted interception of the laser light. Both these consequences of the difference in refractive index must be addressed before comprehensive laser-Doppler measurements of bubbly flow can be undertaken.

Durst & Zaré (1975) first showed that satisfactory LDA signals could be obtained from spherical particles with a diameter in the range 1–10 mm. Wigley (1978) measured the velocity and diameter of water droplets with a diameter in the range 0.1–1 mm. The droplet diameter was inferred from the time interval between glancing-angle reflections and the droplet velocity. Martin *et al.* (1981) measured the characteristics of LDA signals obtained from air bubbles with a diameter range of 0.2–1.0 mm rising in water. A single photomultiplier tube was used and was placed in a forward-scatter arrangement. They observed signals with a triple-peak pedestal instead of the single-peak pedestal observed with particles of 1 μm dia. They attributed the side peaks to the reflection of one of the laser beams off the side of the bubble.

Martin & Chandler (1982) employed the triple-peak signal to measure the diameter and velocity of air bubbles rising in water with a diameter range of 0.1–1 mm. The velocity was inferred from the Doppler frequency of the burst signal. The diameter was inferred from the time interval between the side peaks of the pedestal and the velocity. Their method will be referred to as the triple-peak technique of bubble sizing.

The triple-peak technique was applied by Brankovic *et al.* (1984) to the measurement of bubbles with diameter in the range 0.07–1.20 mm rising singly in a quiescent tank of distilled water. Both carbon dioxide and air bubbles were studied and dynamics and mass transfer data were obtained.

Laser-Doppler measurements of both liquid-phase velocity and bubble velocity were obtained by Durst *et al.* (1984). They did not measure the bubble diameter.

†To whom all correspondence should be addressed.

An alternate method of diameter measurement based on the existence of a spatial fringe pattern has been developed (Durst 1982; Bachalo & Houser 1985). The advantage of the triple-peak technique over the fringe method is that the triple-peak technique employs a single photodetector in a minimally modified standard dual-beam LDA.

Some of the LDA techniques employed to measure a flow containing suspended particles cannot be adapted to measure a bubbly flow. For example, the technique employed by Hamdullahpur *et al.* (1987) requires the surface of the particles to be impregnated with a fluorescent dye so that solid-phase signals can be distinguished from liquid-phase signals.

The successful application of the LDA to the measurement of bubbles depends on both the ability to measure a single bubble and the ability to perform this measurement when there is the possibility of more than one bubble in the optical path. The purpose of this research was to study both of these problems using the triple-peak technique to simultaneously measure the velocity and diameter of a bubble. This was the first application of the technique to the measurement of controlled multiple streams of bubbles rising in a quiescent liquid.

The research reported here was confined to bubble diameters in the range 0.8–1.8 mm. The liquid phase surrounding the spherical bubble has a greater refractive index than the gas phase inside the bubble. The dual-beam type of LDA was considered.

2. APPARATUS AND PROCEDURE

2.1. Test section

The test section was a vertical Plexiglas channel having a rectangular cross section of 87.3 × 47.3 mm inside dimensions and a wall thickness of 6.35 mm. It has an overall height of 520 mm, including a 150 mm long bubble-collection tube. The channel was mounted on a three-dimensional traversing mechanism. The position of the bubble passing through the LDA measuring volume was controlled by moving the channel, with the optical system remaining fixed. The traversing mechanism had a resolution of 10 μm in both the x and y directions, and 5 μm in the z direction. The test section is shown in figure 1.

The nitrogen bubbles were introduced singly through an array of flexible hypodermic needles into the channel containing quiescent distilled water. The needles were each 125 mm long and had an inside diameter of 0.10, 0.15, 0.20 or 0.25 mm. The gas pressure was regulated between 0 and 200 kPa and the flowrate was controlled by micro-metering valves. The inlet gas pressure to the needles was monitored by a pressure transducer. The ambient temperature was 293 K.

A Plexiglas plate, containing an array of small holes of 0.3 mm dia, was located just below the tip of the needles. In multistream experiments, the injection locations of bubbles were controlled by passing the needles through the desired holes in the plate, as shown in figure 1.

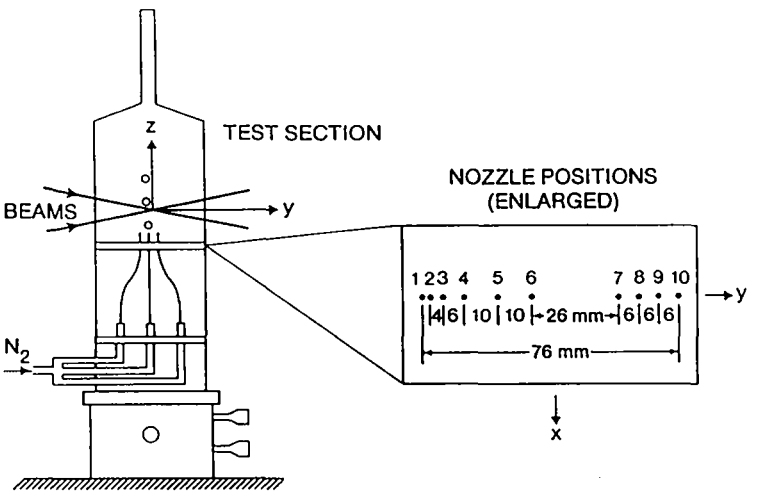

Figure 1. Schematic of the test section.

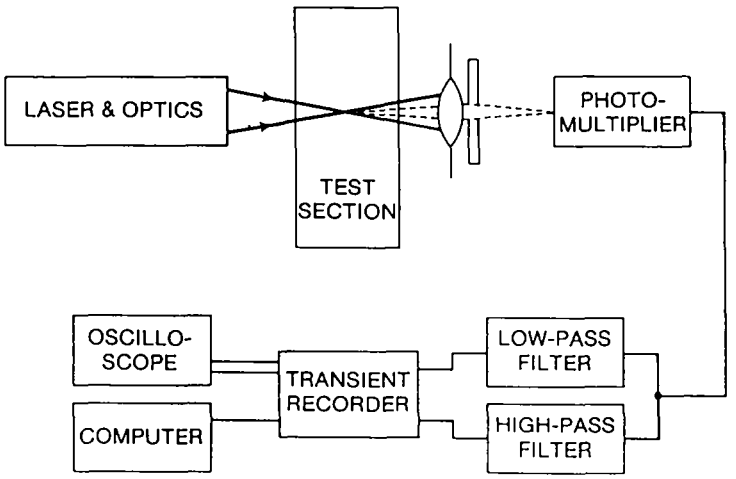

Figure 2. Schematic of the instrumentation.

2.2. Instrumentation

The instrumentation is shown in figure 2. The LDA consisted of a Coherent Innova 90 argon-ion laser with a maximum output power of 2 W and an optical system manufactured by Opto-Electronische Instrumente GmbH. Only the green component of the laser emission, with a wavelength in air of 514.5 nm, was used. The pair of green beams lay in a vertical plane and had a crossing angle $2\alpha_a$ of 5.725° in air. The beams had a crossing angle 2α of 4.294° in water. The collecting optics consisted of a 150 mm focal length lens, an aperture immediately behind the lens and a photomultiplier. The lens was located at about 300 mm from the laser beam measuring volume, with the optical axis passing through its center. The aperture was positioned on the centerline of the collecting lens, 43 mm behind the lens. Its diameter was adjustable between 1 and 25 mm. The photomultiplier assembly had a 0.3 mm dia entrance pinhole and a bandwidth of 0–10 MHz.

The output of the photomultiplier assembly was divided into two channels. The first channel was low-pass filtered to obtain the pedestal component of the Doppler burst. The second channel was high-pass filtered to obtain the Doppler frequency component of the Doppler burst. Both channels were digitized simultaneously by a Datalab 1080 transient recorder. The leading edge of the pedestal was used to trigger the transient recorder. The transient recorder had an analog bandwidth of 0–5 MHz, a maximum sampling rate of 20 MHz/channel, voltage resolution of 1:256 (full scale) and a storage capacity of 4096 samples/channel. It was connected to a PDP-11/23+ computer via an IEEE-488 general-purpose interface bus.

The pedestal component was analyzed first; only those having the characteristic three-peak shape were accepted. The locations and amplitudes of each peak and the time between the maxima of the two side peaks were evaluated using the computer software and the technique of Martin & Chandler (1982). The time between the maxima of the two side peaks represented the bubble transit time Δt. The program then analyzed the Doppler frequency component of the signal and found the frequency of each peak using a zero-crossing algorithm similar to the one employed by Durst & Tropea (1977). Several signal validation tests were performed on each Doppler burst. The program computed the bubble velocity U_b from the frequency of the center peak f_D using

$$U_b = f_D \frac{\lambda}{2 \sin \alpha_a}. \quad [1]$$

It then computed the bubble diameter from the transit time and the velocity using

$$D(y) = U_b \Delta t. \quad [2]$$

A total of 50 valid bursts, which satisfied all discrimination criteria, were sampled and the mean and standard deviation of the velocity and diameter were evaluated.

Program options were available to minimize the time required to perform a particular experimental task. For example, in studying the effect of interception of laser light by other bubbles,

only the pedestal component of the signal was recorded and analyzed. This allows a much higher bubble flowrate to be processed on a on-line basis.

2.3. Testing the instrumentation with a model air bubble

The instrumentation was tested with a model air bubble. This model consisted of a spherical air bubble of 3.59 mm dia embedded in a rectangular block of transparent silicone elastomer (Varty 1986). It was mounted on a motorized rotating disk which was on the top of the three-dimensional traversing mechanism. The model moved through the LDA measuring volume in the same manner as a rising bubble. The signals obtained from the model air bubble were useful because they were independent of the flow in the test section.

2.4. Independent measurement of bubble size

The design of the test section provided the capability of performing independent bubble-size measurements. A closed bubble-collection tube was located at the top of the test section, as shown in figure 1. In each experiment, a total volume of 1–2 cm^3 of water was displaced from this tube and the total number of bubbles collected was counted. Typically, 2000 bubbles were required to displace 1 cm^3 of water from the test section. The transient recorder was operated at a low sampling rate and the signal from each bubble was recorded as a pulse. The number of bubbles counted was continuously displayed on the computer terminal. The bubble diameter was calculated from the total volume collected and the number of bubbles counted. The same procedure was repeated several times and then the mean and standard deviation of bubble diameter were calculated. The compressibility of the gas was negligible.

2.5. Measurement of bubble-detection region

The bubble-detection region was defined as the region of the xy plane within which a three-peak LDA signal was obtained from a bubble rising in the z direction. It was possible to retrieve the information about any bubble as long as its center coordinates, on the xy plane, were within the bubble-detection region. Bubbles were injected from a single hypodermic needle. The origin of the xyz coordinate system was fixed 20 mm above the needle's tip. The bubble-detection region was measured by moving the needle to various horizontal positions.

The LDA measuring volume was defined as the region containing the origin of the xyz coordinate system within which the irradiance of laser light was $\geqslant e^{-2}$ of the irradiance at the origin; the origin was the point of maximum irradiance. The value of e^{-2} is approx. 0.135. The LDA measuring volume was disrupted by the passage of bubbles through it. Therefore, the bubble-detection region was a more useful concept in these experiments.

The center of the LDA measuring volume was determined as follows. The hypodermic needle was raised vertically, intersecting the measuring volume. The needle was then moved in the x and y directions until it appeared to be at the center of the measuring volume. Then the needle was lowered back to where the experiments required, and the bubbles were introduced. Fine adjustment of the needle's position was performed until the signal amplitude was a maximum and the signal shape was symmetric. This location was recorded as $x = y = 0$ and was considered as the center of the LDA measuring volume.

The bubble-detection region was evaluated by moving the needle in the y direction for various fixed x values. Also, the effect of the bubble center coordinates on the signal characteristics, measured bubble size and velocity were obtained. A total of 50 Doppler bursts were sampled at each measuring point, providing statistically stable results. The Doppler frequency f_D was in the approximate range 40–55 kHz. The pedestal component was obtained by low-pass filtering the signal from the photomultiplier assembly at 100 Hz. The Doppler frequency component was obtained by band-pass filtering the signal between 20 and 100 kHz. Both channels were digitized at a rate of 500 kHz for 4096 samples/channel. The trigger level was set just above the noise level of the pedestal signals.

2.6. Effect of interception of laser light by other bubbles

The arrangement of hypodermic needles used in the experiments is shown schematically in figure 1. A selected hypodermic needle, called the center nozzle, was used. It was positioned so that

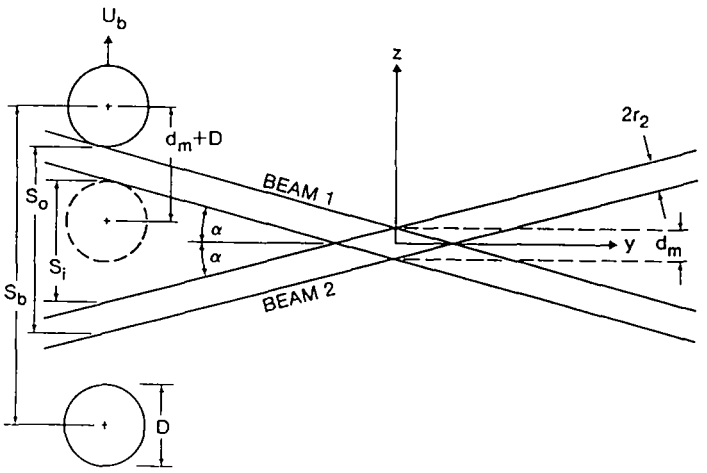

Figure 3. Interception of laser light by other bubbles.

the bubbles would pass through the center of the measuring volume. Up to seven other hypodermic needles, called side nozzles, were also used. They were used to introduce bubbles which were outside the bubble-detection region, but which crossed the optical (y) axis. These side bubbles would intercept the laser beams and/or the scattered light from the center nozzle's bubbles. The locations and bubble flowrates of both the center and side nozzles were varied and the effect on the interception of laser light was studied.

The effect of interception of laser light by other bubbles was indicated by the valid burst ratio N_{VBR}, which was defined as the ratio of the number of bursts having a characteristic triple-peak shape to the total number of bursts recorded. Without any interference, the valid burst ratio would be 100%.

The interception of laser light by other bubbles is shown schematically in figure 3. A statistical analysis of this phenomenon was performed; the details are given in the appendix. This analysis predicted that when the side streams are on the laser side of the measuring volume ($y < 0$), the probability of detecting a valid signal is

$$P_D = 1 - 2\left(\frac{2r_2}{\cos\alpha} + D\right)\frac{Q_b}{U_b}, \qquad [3]$$

where r_2 is the beam radius and Q_b is the total bubble flowrate of the side nozzles. The value of r_2 was 0.137 mm. The analysis also predicted that when the side streams are on the photomultiplier side of the measuring volume ($y > 0$), the probability of detecting a valid signal is

$$P_D = 1 - \left(\frac{2r_2}{\cos\alpha} + D\right)\frac{Q_b}{U_b}. \qquad [4]$$

The bubble diameter and velocity were evaluated for each nozzle before starting each experiment. Only the pedestal components of the signals were digitized in this set of experiments, with a sampling interval of 29.7 μs and 256 samples/Doppler burst. These sampling values were chosen to minimize the time required for each test. A total of 100 bursts were sampled in each test to give the valid burst ratio. Twenty tests were performed in each experiment to obtain the mean and standard deviation of the valid burst ratio. This produced statistically stable results.

3. RESULTS AND DISCUSSION

3.1. Model air bubble

Two separate experiments were performed with the model air bubble; the only difference between them was the velocity of the rotating disk. The bubble velocities were 175.0 and 277.0 mm/s. The relative error of the velocity measured by the LDA was $\pm 0.5\%$. The relative error of the diameter

Table 1. Details of the single-stream experiments

Experiment	Bubble diameter, D (mm)	Bubble velocity, U_b (m/s)	Reynolds number, Re	Eotvos number, Eo
A	0.853	0.2804	177	0.098
B	1.390	0.2591	359	0.260
C	1.500	0.2797	419	0.303
D	1.688	0.2814	474	0.383
E	1.824	0.2830	515	0.447

measured by the LDA was $\pm 0.4\%$. These relative errors were calculated using the measured disk rotation and the measured size of the model air bubble as reference values.

3.2. *Single stream of bubbles*

Five experiments were performed with a single nozzle generating a single stream of bubbles, as shown in table 1. The Reynolds number is given by $\mathrm{Re} = \rho D U_b/\mu$, where ρ is the density of the water and μ is the viscosity of the water. The Eotvos number is $\mathrm{Eo} = g\,\Delta\rho D^2/\sigma$, where g is the acceleration due to gravity, $\Delta\rho$ is the density difference between the water and nitrogen and σ is the surface tension. The effect of the x and y coordinates of the bubble center on the measured Doppler frequency, transit time and other signal characteristics were studied. A typical signal is shown in figure 4.

The Doppler frequency, and hence the measured bubble velocity, was independent of the bubble-center y coordinate. The transit time, and hence the measured bubble diameter, was dependent on the bubble-center y coordinate, as shown in figure 5. The bubble diameter $D(y)$ was calculated from the bubble velocity U_b and the transit time Δt using [2]. From geometric optics, the relationship between $D(y)$ and the actual bubble diameter D is

$$D(y) \approx D + 2y \tan\alpha, \qquad [5]$$

where α is the beam crossing half-angle. The line drawn in figure 5 was obtained from [5]. It only agrees qualitatively with the data. There is a systematic error of 0–10% in the measured diameter.

The measured bubble velocity and measured bubble diameter were independent of the x coordinate of the center of the bubble.

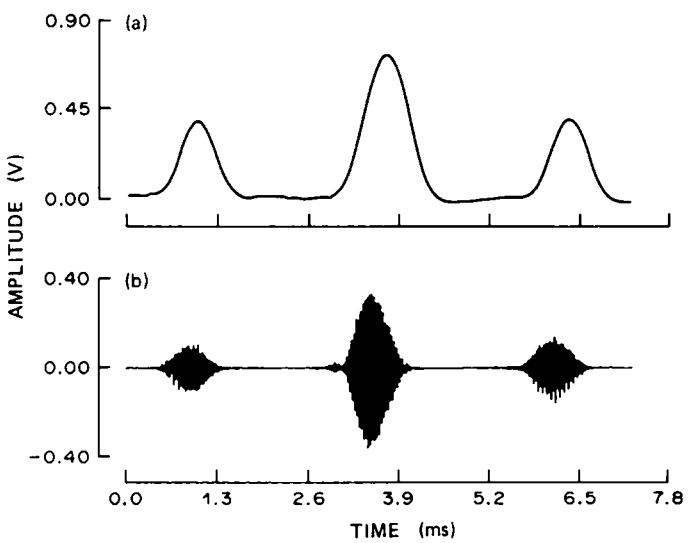

Figure 4. Typical triple-peak LDA signal at $(x, y) = (0, 0)$: (a) pedestal component; (b) Doppler component.

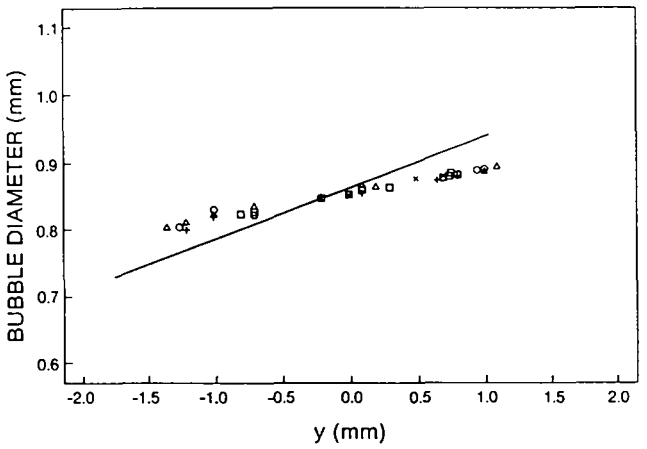

Figure 5. Measured bubble diameter as a function of the bubble-center y coordinate (experiment A): □, $x = -0.04$ mm; ○, $x = -0.02$ mm; △, $x = 0.00$ mm; +, $x = 0.02$ mm; ×, $x = 0.04$ mm. The line represents [5].

The observed bubble-detection regions are shown in figure 6. For each experiment, the data points along the perimeter of the bubble-detection region were plotted in this figure. The data points in this figure represent valid triple-peak signals. The data points inside the bubble-detection regions, which represent valid triple-peak signals, were not plotted in this figure. The data points outside the bubble-detection regions, representing invalid signals, also were not plotted. The bubble-detection regions were symmetric with respect to the x axis and asymmetric with respect to the y axis. The bubble-detection region was approximately elliptical in the xy plane and its length in both x and y directions was proportional to bubble diameter. Hence, the area of this region in the xy plane was $A \approx 0.25D^2$. The spatial resolution decreased with increasing bubble diameter.

The LDA measuring volume, defined by the e^{-2} points of the irradiance distribution, had calculated lengths of $h_m = 0.27$ mm in the x direction and $l_m = 7.3$ mm in the y direction. Therefore, the bubble-detection region was smaller than the LDA measuring volume for the bubble diameters used in these experiments. Also, the center of the bubble-detection region was offset from the origin of the coordinate system, whereas the center of the LDA measuring volume coincided with the origin. These results show that the region from which bubble signals were obtained differs from the region from which liquid-phase signals could be obtained.

The length of the bubble-detection region in the z direction was not measured. The calculated length of the LDA measuring volume in the z direction d_m was 0.27 mm. The quantity $d_m + D$ would be an upper bound on the length of the bubble-detection region in the z direction.

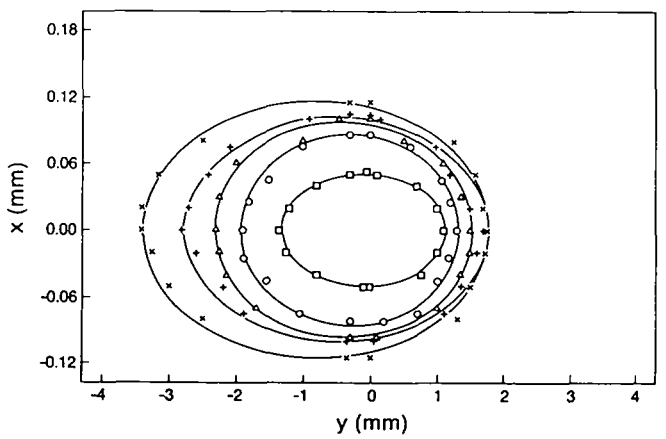

Figure 6. Bubble-detection regions (experiments A–E): □, A; ○, B; △, C; +, D; ×, E. The ellipses were fitted to the data.

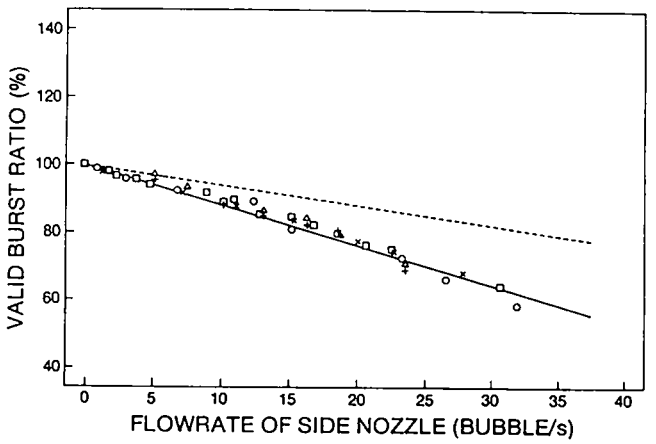

Figure 7. Valid burst ratio with one side nozzle (SN): □, SN No. 3, $Q_c = 2.50$ bubbles/s, $\Delta t = 0.00700$ s; ○, SN No. 1, $Q_c = 4.11$ bubble/s, $\Delta t = 0.00551$ s; △, SN No. 1, $Q_c = 5.59$ bubble/s, $\Delta t = 0.00585$ s; +, SN No. 1, $Q_c = 5.59$ bubble/s, $\Delta t = 0.00633$ s; ×, SN No. 2, $Q_c = 4.11$ bubble/s, $\Delta t = 0.00550$ s. The center nozzle (CN) was located at position 6. ——— represents [3]; — — — represents [4].

3.3. *Multiple streams of bubbles*

Two different sets of experiments were performed:

(1) Experiments with a single side stream of bubbles.
(2) Experiments with multiple side streams of bubbles.

Bubbles with a 1.5 mm dia were used in all of these experiments. The value of D/U_b was 0.005 s and was equivalent to the bubble transit time.

The form of [3] and [4] suggested that the experimental data should be a function of Q_b only, since r_2, α, D and U_b were fixed during these experiments. A typical graph of the valid burst ratio N_{VBR} vs Q_b is shown in figure 7. A single side nozzle was used to generate a side stream of bubbles at five positions between the laser and the measuring volume. The measured points lie close to the line of [3], as expected. A graph obtained with two side nozzles at three different positions is shown in figure 8. The measured points lie close to the line of [3]. The points obtained with both side streams between the measuring volume and the photomultiplier were expected to follow [4] rather than [3]. A graph obtained with 1–7 side nozzles at various positions is shown in figure 9. Again, the measured points lie close to the line of [3]. Therefore, all of the data were approximated by

$$N_{VBR} = 1 - K_N Q_b, \qquad [6]$$

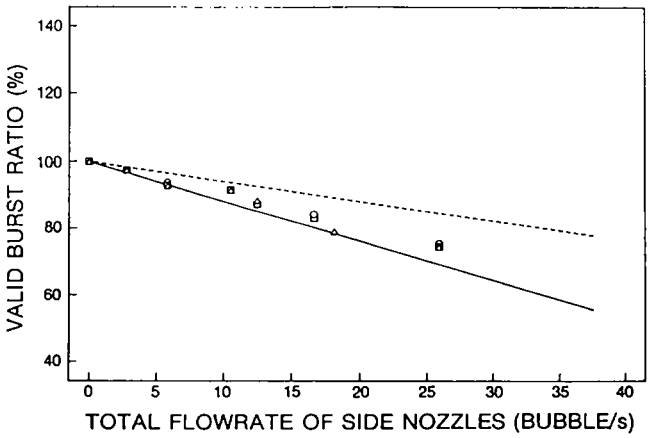

Figure 8. Valid burst ratio with two side nozzles: □, SN Nos 2, 10, CN No. 6; ○, SN Nos 6, 10, CN No. 2; △, SN Nos 2, 6, CN No. 10. $Q_c = 8.33$ bubble/s, $\Delta t = 0.00607$ s. ——— represents [3]; — — — represents [4].

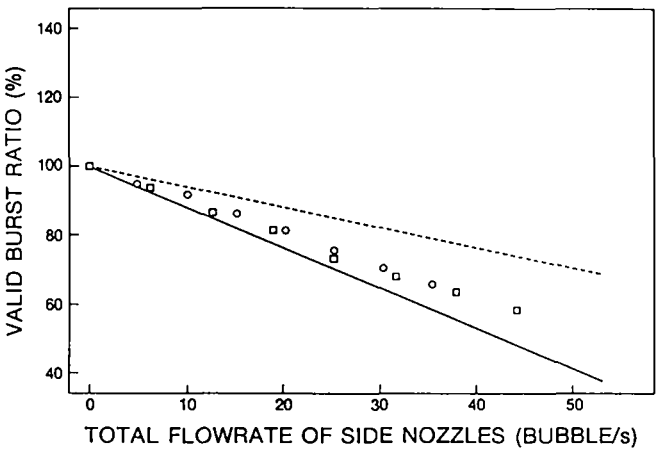

Figure 9. Valid burst ratio with 1–7 side nozzles: □, all SN on laser side of CN No. 10, $Q_{bl} = 6.25$ bubble/s, $Q_c = 5.83$ bubble/s; ○, all SN on photomultiplier side of CN No. 1, $Q_{bl} = 5.00$ bubble/s, $Q_c = 5.00$ bubble/s. ——— represents [3]; — — — represents [4].

with $K_N = 0.011$ s calculated from the constant factors in the second term of [3]. It was found that K_N remained constant and was independent of the number and location of the side nozzles.

The statistical analysis predicted some features of the experimental data such as the linear graphs and the independence of the center nozzle flowrate. However, the statistical analysis did not explain why the placement of nozzles on the laser side of the center nozzle produced the same effect as the placement of nozzles on the photomultiplier side of the center nozzle.

Using the measured length of the bubble-detection region in the x direction as the thickness of the bubbly-flow field, an equivalent void fraction was estimated and found to be proportional to the flowrate of the side nozzles. Hence, the valid burst ratio decreased linearly with void fraction to a value of 60% at a void fraction of 0.012.

3.4. Computer simulation

A set of computer programs was written to simulate the LDA signal. The computer simulation was based on geometric optics. The geometric-optics principles (van de Hulst 1981) were employed by Davis (1955) to solve the problem of a bubble uniformly illuminated by a plane electromagnetic wave. The present problem involves a bubble partly illuminated by a Gaussian laser beam, which is considerably more complex. In this investigation, with the bubble diameter $2R$ in the range of 0.85–1.83 mm, the Mie parameter $2\pi R/\lambda$ was in the range 5200–11,200. These large values of the Mie parameter justified the geometric-optics approach, in which diffraction is neglected.

Other assumptions used in the programs included: (1) the bubble is spherical and homogeneous; (2) the bubble trajectory is parallel to the z axis; and (3) the bubble does not rotate.

A series of computer runs with a bubble diameter of 1.5 mm were carried out and the results were compared with those from experiment C. The computer results indicated that the size of the bubble-detection region is independent of bubble diameter, contrary to the experimental results. The computer results predicted a larger shift of the center of the region along the negative y axis with increasing bubble diameter than the observed shift. Computer-generated triple-peak pedestal signals were compared with the experimental signals, such as the one shown in figure 4(a). The ratio of the maximum amplitude of the center peak P_{cp} to the maximum amplitude of the side peak P_{sp} was $P_{cp}/P_{sp} \approx 18$ for the computer results and $P_{cp}/P_{sp} \approx 2$ for the experimental results.

3.5. Implications for measuring liquid-phase velocity

The liquid-phase velocity was not measured. However, it can be measured by using the light scattered from particles with diameters of the order of 1 μm which can be suspended in the liquid. This is the basis of LDA measurements of single-phase flow. The amplitude discrimination technique described by Durst (1982) may be used to distinguish the bubble signals from the liquid-phase ones. A signal having an amplitude larger than a threshold level is regarded as a

bubble signal, whereas one with an amplitude smaller than this level is regarded as a liquid-phase signal. This threshold level must be chosen to ensure correct identification. The signal amplitude resulting from a 1 mm dia bubble passing through the center of the LDA measuring volume is several orders of magnitude greater than that of a 1 μm particle following the same trajectory. However, the observations suggest that a bubble passing near the edge of the LDA measuring volume produces a lower-amplitude signal without side peaks which could be identified as a liquid-phase signal.

3.6. Further discussion

It has been suggested that the successful application of the LDA to the measurement of bubbles depends on both the ability to measure a single bubble and the ability to perform this measurement when there is more than one bubble in the optical path. The present results provide information for the triple-peak technique applied to a particular type of flow. One might ask whether these results could be applied to a different type of flow.

The measurement of the model air bubble showed that the effect of the y coordinate of the bubble center on the measured velocity and diameter was similar to the effect observed with the gas bubbles in water. Therefore, the results shown in figure 5 would apply to another flow.

The side peaks and the center peak obtained from the model air bubble had the same Doppler frequency. The side peaks and center peak obtained from a gas bubble in water had different Doppler frequencies. This agrees with the results of Brankovic *et al.* (1984), who suggested that the bubbles are ellipsoidal in shape and oscillate about a mean diameter as they rise above the nozzle. The bubbles appeared to be spherical. However, the combination of Reynolds number and Eotvos number encountered suggests (Clift *et al.* 1978) that the larger bubbles in experiments B to E would be ellipsoidal and would exhibit oscillations in shape and a non-rectilinear trajectory when they reach their terminal velocity. The present measurements were obtained 20 mm above the tip of the nozzle. The results of Brankovic *et al.* (1984) suggest that the bubbles in the present experiments would not have reached their terminal velocity.

When the measurements were analyzed, it was assumed that the bubbles were spherical and followed a vertical trajectory. The effect of non-spherical bubbles was not estimated because of the problems with the geometric-optics calculations. The effect of non-vertical trajectories was not estimated because the paths of individual bubbles were not measured. Since the measurements were obtained near the tip of the nozzle, the departure from a vertical trajectory may have been small.

The upward motion of each bubble would induce motion of the liquid, affecting the motion of bubbles in the same stream and in adjacent streams. For the data shown in figures 5–9, the minimum vertical distance between bubbles was 34 mm. For the data shown in figures 7 and 8, the minimum horizontal distance between nozzles was 26 mm. These distances were much larger than the bubble diameter of 1.5 mm. The maximum value of the average volumetric flux of gas for the test section was 0.0213 mm/s; it was encountered for the data of figure 9. This flux was much smaller than the bubble velocity of 279.7 mm/s. Thus, the interaction between bubbles may have been small.

The results shown in figures 6–9 should be applied cautiously to another flow because of the possible effects of the shape and trajectory of bubbles on the present results.

4. CONCLUSIONS

The triple-peak technique provided reliable measurements of bubble velocity which were independent of the bubble-center coordinates. The measured bubble diameter was independent of the bubble-center x coordinate, but varied linearly along the optical axis y. This introduces an error which may limit the application of the triple-peak technique. The area of the bubble-detection region in the xy plane was proportional to the square of the bubble diameter.

The multiple stream experiments showed that the probability of detecting a valid signal is independent of the locations and number of bubble streams. The probability of detecting a valid signal decreased linearly with increasing total bubble flowrate of the side nozzles.

The most significant results were the cross-sectional area of the bubble-detection region and the dependence of valid burst ratio on bubble flowrate. The measurements of cross-sectional area provide the spatial resolution of the triple-peak technique and could permit the extension of the technique to the measurement of void fraction. The measurements of valid burst ratio suggest that this is possible when the void fraction is $\leqslant 0.01$.

Acknowledgements—This research was supported by the Natural Sciences and Engineering Research Council of Canada through Grants U0321 and A6015. This research was originally part of a thesis at the University of Toronto (Yu 1986).

REFERENCES

BACHALO, W. D. & HOUSER, M. J. 1985 Experiments in polydisperse two-phase turbulent flows. In *International Symposium on Laser Anemometry*, FED-Vol. 33, pp. 135–141. ASME, New York.

BRANKOVIC, A., CURRIE, I. G. & MARTIN, W. W. 1984 Laser-Doppler measurements of bubble dynamics. *Phys. Fluids* **27,** 348–355.

CLIFT, R., GRACE, J. R. & WEBER, M. E. 1978 *Bubbles, Drops and Particles*. Academic Press, New York.

DAVIS, G. E. 1955 Scattering of light by an air bubble in water. *J. opt. Soc. Am.* **45,** 572–581.

DURST, F. 1982 Combined measurements of particle velocities, size distributions and concentrations. *Trans. ASME Jl Fluids Engng* **104,** 284–296.

DURST, F. & TROPEA, C. 1977 Processing of laser-Doppler signals by means of a transient recorder and a digital computer. Report SFB80/E/118, Univ. of Karlsruhe, F.R.G.

DURST, F. & ZARÉ, M. 1975 Laser Doppler measurements in two phase flows. Report SFB80/TM/63, Univ. of Karlsruhe, F.R.G.

DURST, F., TAYLOR, A. M. K. P. & WHITELAW, J. H. 1984 Experimental and numerical investigation of bubble-driven laminar flow in an axisymmetric vessel. *Int. J. Multiphase Flow* **10,** 557–569.

HAMDULLAHPUR, F., PEGG, M. J. & MACKAY, G. D. M. 1987 A laser-fluorescence technique for turbulent two-phase flow measurements. *Int. J. Multiphase Flow* **13,** 379–385.

VAN DE HULST, H. 1981 *Light Scattering by Small Particles*. Dover, New York.

MARTIN, W. W. & CHANDLER, G. M. 1982 The local measurement of the size and velocity of bubbles rising in liquids. *Appl. scient. Res.* **38,** 239–246.

MARTIN, W. W., ABDELMESSIH, A. H., LISKA, J. J. & DURST, F. 1981 Characteristics of laser-Doppler signals from bubbles. *Int. J. Multiphase Flow* **7,** 439–460.

VARTY, R. L. 1986 Fringe method of bubble sizing using a laser-Doppler anemometer. *J. Phys. E: Scient. Instrum.* **19,** 858–863.

WIGLEY, G. 1978 The sizing of large droplets by laser anemometry. *J. Phys. E: Scient. Instrum.* **11,** 639–642.

YU, P. Y. W. 1986 Feasibility study of the triple-peak LDA technique on bubbly two-phase flow. M.A.Sc. Thesis, Dept of Mechanical Engineering, Univ. of Toronto, Ontario.

APPENDIX

The interception of laser light by other bubbles can be divided into two cases: (1) the side stream of bubbles is between the laser and the measuring volume; and (2) the side stream of bubbles is between the measuring volume and the photomultiplier. In the first case, laser light is intercepted before it reaches the bubble passing through the measuring volume. In the second case, laser light is intercepted after it is scattered from the bubble passing through the measuring volume.

In the first case, consider a side stream of bubbles as shown in figure 3. The bubbles are produced at a rate of Q_b and rise at a velocity U_b. The separation between bubble centers is $S_b = U_b/Q_b$. Let P_T be the probability of interception of the beams by a bubble in the side stream. Let P_b be the probability of interception of a single beam by a bubble in the side stream and let P_m be the probability of simultaneous interception of both beams by bubbles in the side stream. Then

$P_T = 2P_b - P_m$. The probability of detecting a valid signal is $P_D = 1 - P_T = 1 - 2P_b + P_m$. These probabilities are computed from the time intervals in which these events occur. Let S_o be the outer separation between the beams, as shown in figure 3. Assume that $D < S_i$. Then the same bubble never touches both beams at the same time. Assume that $S_b - D > S_o$. Then two different bubbles never touch different beams at the same time. Thus,

$$P_D = 1 - 2P_b. \qquad [A.1]$$

The probability P_b is computed from the fraction of time that a beam is intercepted by a bubble:

$$P_b = \frac{\dfrac{(d_m + D)}{U_b}}{\dfrac{1}{Q_b}} = (d_m + D)\frac{Q_b}{U_b}. \qquad [A.2]$$

The distance across the beam in the z direction, d_m, is based on the e^{-2} points of the irradiance distribution. It is calculated from the e^{-2} beam radius r_2 using

$$d_m = \frac{2r_2}{\cos \alpha}. \qquad [A.3]$$

Combining [A.1]–[A.3] gives [3]. It is also possible to derive formulas in which the two inequalities $D < S_i$ and $S_b - D > S_o$ are not satisfied. However, these two inequalities were satisfied in all experiments reported here.

In the second case, the bubble passing through the measuring volume scatters the incident laser beams so that part of them is directed towards the photomultiplier. At the same time, the scattered laser light can be intercepted by a bubble in the side stream between the measuring volume and the photomultiplier. It is assumed that the scattered light traveling to the photomultiplier is confined to a cylinder of diameter d_m coaxial with the positive y axis, as shown in figure 3. The analysis is the same as the first case, except that here a single beam of light is considered. Hence, [4] can be derived. The assumption that the scattered light is confined to the cylinder described above must be considered only as an approximation.

Equation [3] can be used when more than one side stream of bubbles satisfies $y < 0$, $D < S_i$ and $S_b - D > S_o$. The total bubble flowrate of the side nozzles Q_b is the sum of the individual bubble flowrates of each side nozzle, Q_{bi}. Equation [4] can be used when more than one side stream of bubbles satisfies $y > 0$. Equations [3] and [4] are valid for multiple side streams of bubbles because the probabilities of interception for each side stream are independent and therefore additive.